



Cite this: *RSC Adv.*, 2025, **15**, 30552

A novel sensitive electrode based on a chitosan/rGO/CuO composite for the detection of urea concentration

Irwana Nainggolan, ^{a,b,c} Ardiansyah Sembiring, ^{abc} Tulus Ikhsan Nasution, ^{cd} Rahmadhani Banurea, ^d Reka Mustika Sari, ^e Andriayani, ^a Rozyanty Rahman, ^f Bing Li, ^g Rica Asrosa ^d and Khatarina Meldawati Pasaribu ^h

Chitosan/reduced graphene oxide/copper oxide (CS/rGO/CuO) films were successfully deposited on a screen-printed electrode (SPE) surface by applying the electrodeposition technique and were utilized in detecting urea concentration using cyclic voltammetry (CV). The current study presents a novel sensitive electrode based on CS/rGO/CuO used to detect urea fertilizer. The characterization of the prepared samples was conducted using FTIR, XRD, and cyclic voltammetry. FTIR and XRD analyses confirmed that rGO and CuO were successfully dispersed in the CS matrix. The FE-SEM morphology showed a slight agglomeration, which was caused by physical interaction among CS, rGO and CuO. The CS/rGO/CuO-modified SPE had an increased electrochemical performance compared with the CS-modified SPE. Our reported study revealed that the CS/rGO/CuO 0.8%-modified SPE has extremely promising electrochemical performance. The sensing properties of CS/rGO/CuO in various concentrations of urea were studied using CV. In this study, the obtained sensitivity and *R*-square (R^2) values were $1.93 \times 10^{-3} \mu\text{A} \mu\text{M}^{-1} \text{cm}^{-2}$ and 0.9599, respectively. In addition, the observed electrocatalytic current had a limit of detection of $0.14 \mu\text{M}$ and a limit of quantification of $0.49 \mu\text{M}$. These results indicate that the CS/rGO/CuO-modified SPE can be used to detect urea concentration, in which the addition of CuO concentration contributes significantly to the sensing properties of the resulting modified electrodes.

Received 29th November 2024
 Accepted 22nd July 2025

DOI: 10.1039/d4ra08451a
rsc.li/rsc-advances

1. Introduction

Currently, in the field of agriculture, the development of advanced and modern technologies continues to enhance agricultural productivity and sustainable crop quality. One of the key methods for these is the application of fertilizers.¹ Fertilizer application to plants is considered the most important factor for improving the soil's physical, chemical, and

biological characteristics, leading to the desired harvest results.² Urea fertilizer possesses crucial significance in the agricultural sector.³

Urea fertilizer, known as a nitrogen fertilizer, containing approximately 46% nitrogen, exhibits excellent solubility in water, and it is easily absorbed by plants, making it a very efficient nitrogen source for plants.⁴ Urea fertilizer is an organic compound with a carbonyl group (C=O) attached to two NH₂ groups.⁵ A deficiency of urea fertilizer in plants can result in slow growth, yellowing of leaves, reduced leaf production, lower crop yields, and increased susceptibility to diseases, as previously reported by Balitbangtan (2019).⁶ The standard usage of urea fertilizer ranges from 1.5% to 4.5% depending on the type of plant.³ However, many farmers are not aware about the precise application of fertilizer to plants, and they sometimes apply excessive amounts of fertilizer. Consequently, this can cause harmful effects on the environment, such as damages to soil ecosystems, microorganism elimination, water pollution,⁶ greenhouse gas emissions, and surface water eutrophication.⁷ Therefore, alternative innovations are needed for detecting urea concentration.

Several approaches have been employed for both the quantitative and qualitative examination of urea concentrations. The

^aDepartment of Chemistry, Faculty of Mathematics and Natural Science, Universitas Sumatera Utara, Medan, 20155, Indonesia. E-mail: irwana@usu.ac.id

^bCenter of Excellent Chitosan and Advance Materials, Universitas Sumatera Utara, 20155, Medan, Indonesia

^cCenter of Excellent for Greenhouse Gas Emission Control, Universitas Sumatera Utara, 20155, Medan, Indonesia

^dDepartment of Physics, Faculty of Mathematics and Natural Science, Universitas Sumatera Utara, Medan, 20155, Sumatera Utara, Indonesia

^eResearch Center for Food Technology and Processing, National Research and Innovation Agency, Gunungkidul, Yogyakarta, Indonesia

^fSchool of Materials Engineering, Faculty of Chemical Engineering Technology, Universiti Malaysia Perlis, Malaysia

^gInstitute for Materials Discovery, University College London, London, WC1E 7JE, UK

^hResearch Center for Biomass and Bioproducts, National Research and Innovation Agency of Indonesia (BRIN), Cibinong 16911, Indonesia



determination is commonly conducted by Kjeldahl titration, conductometry, or high-performance liquid chromatography (HPLC) analysis. However, these approaches are toxic, time-consuming, and costly.⁷⁻⁹ A urea fertilizer sensor was also reported to determine the concentration of urea. However, it currently lacks adequate sensitivity and selectivity, and it exhibits instability during the process of analysis.¹⁰ Therefore, it is necessary to develop a straightforward, cost-effective, and uncomplicated technique that can provide high sensitivity and accurate detection.

Over the past ten years, electrochemical techniques have developed as a highly sensitive and less time-consuming approach, and they do not necessitate advanced instrumentation.¹¹ Electrochemical techniques, specifically voltammetric and amperometric methods, exhibit high levels of precision. The preparation of their electrodes is simple.¹² Cyclic voltammetry (CV) has been utilised to report almost all chemical detections. In this process, it measures the current produced through a series of 3 electrodes (working, reference, and auxiliary) when voltage is applied. The resulting redox current potential is interpreted as the measured sample concentration.^{13,14} However, the working electrode's surface modification is the primary factor influencing the sensitivity and selectivity of CV. Until now, the use of nanomaterials has become popular to modify the working electrode's surface.¹⁵

Many researchers have utilized metal oxides, such as zinc oxide (ZnO),^{16,17} titanium dioxide (TiO₂),¹⁸ tin oxide (SnO₂),^{19,20} and bismuth oxide (Bi₂O₃),^{21,22} owing to their enormous surface area, flexibility, high stability, and efficient functionalization with carbonyl and hydroxyl groups. CuO, an inorganic material, has been frequently utilised in chemical sensors. Recently, CuO was successfully employed as a modifier in the working electrode of CV owing to its excellent bio-compatibility, acid-base characteristics, and chemical stability.^{23,24} Despite the numerous potential applications of CuO, it is limited by its brittle structure, conductivity, and weak catalytic activity. The addition of graphene is needed to increase CuO's efficiency.

Graphene of reduced graphene oxide (rGO) is known as carbon-based particles with a size of less than 10 nm.²⁵ In general, rGO is a thin-layer nanoparticle consisting of sp²-hybridized carbon. rGO has interesting properties, including a specific surface area, good solubility in water, high biocompatibility, low toxicity, stability at high temperatures, and good conductivity.²⁶ These characteristics enable rGO in several applications, such as chemical sensors, catalytic activity, and energy devices.²⁷ Besides, the use of nanoscale materials has more advantages in many applications.

In the present study, the working electrode was created by modifying the Screen-Printed Electrodes (SPE) using CuO/rGO. The electrodeposition technique is applied. This approach offers numerous benefits owing to its efficiency, simplicity, affordability, and utilization of an electrochemical process (Sembiring *et al.*, 2023).²⁸ Despite these advantages, the use of CuO/rGO composite deposited on the surface of SPE has weaknesses owing to its low film-forming and adhesion properties, making it difficult to adhere to the SPE's surface.

Several materials that can be used to overcome these problems are polyaniline, polypyrrole, polyvinyl alcohol, alginate, cellulose and its derivatives, gelatin, and chitosan. However, chitosan (CS) was chosen to address these weaknesses because it is a renewable cationic polysaccharide, serves as an ion exchanger and has a highly reactive chemical nature. These properties allow CS to generate hydrogen bonds between nitrogen in NH₂⁻ bonds of CS and NH₂⁻ bonds on urea.²⁹ In addition, CS offers excellent film-forming capacity and good adhesion properties.³⁰ Moreover, electrochemical-based chitosan for urea detection provides some advantages, such as high biocompatibility, good enzyme immobilization ability, improved sensor sensitivity, and modification ability with nanomaterials. Additionally, the hydrophilic and adhesive properties of CS aid in stabilizing the electrochemical system during the measurement process. Thus, the incorporation of these three materials can mutually support each other as sensitive materials for the SPE's working electrode to detect urea fertilizer. The structural, morphological, and electrochemical characteristics of the CS/CuO/rGO-modified electrode are discussed.

2. Experimental

2.1 Materials

All reagents and chemicals, such as chitosan powder, reduced graphene oxide (rGO), copper oxide (CuO), phosphate saline buffer (PBS) pH 7, acetic acid glacial (CH₃COOH), urea, ethanol 96%, and distilled water used in this work were utilized as received and were of analytical grade Merck quality. The screen-printed electrode (SPE) was purchased from CV. Al-Tronic, Medan.

2.2 Preparation of chitosan/rGO/CuO-based electrode

The procedure was performed as reported by Nainggolan *et al.* (2024) with some modifications.³⁰ First, an amount of CS (1.5 g) was introduced into 100 mL of CH₃COOH 2% v/v and stirred for 24 h. Subsequently, 25 mL of rGO 250 ppm and 25 mL of CuO 0.2% (g L⁻¹) were mixed under constant stirring for 2 h at 200–300 rpm. The same treatment was done with varying concentrations of CuO (0.4%, 0.6%, 0.8%, and 1.0%). The concentration of rGO 250 ppm was chosen because of the previous study reported by Sembiring *et al.* (2023).²⁸ Furthermore, 25 mL of CuO/rGO solution was added into 25 mL of CS solution, followed by stirring for 12 h at ambient temperature using a magnetic stirrer. Next, SPE was cleaned using distilled water, followed by an ethanol solution. Before fabricating the modified electrode, a sample test was prepared by creating a urea solution. The urea solution was created with several concentrations, specifically 0.5–3.5 ppm with an increment of 0.5 ppm in PBS solution (pH 7). This refers to the concentration of urea fertilizer, which is required by the plant species, as reported by FAO (2005).³ To make a sensitive working electrode to detect urea fertilizer, a brief electrodeposition apparatus was prepared. Furthermore, SPE electrodes were clamped between the cathode and anode sides. A total of 25 mL of CS/rGO/CuO



solution was placed into the beaker glass. After that, the SPE electrode was dipped into the CS/rGO/CuO solution and then given a current with a voltage of 2.5 volts. The process was conducted for 5 minutes. The modified electrode was subjected to drying at 60 °C for 30 minutes in an oven. Furthermore, the CS/rGO/CuO-modified SPE electrode obtained was characterized using Fourier Transform Infra-Red/FTIR (Shimadzu IR Prestige 21), X-ray Diffraction/XRD (Shimadzu XRD-6100), and Field Emission-Scanning Electron Microscopy/FE-SEM (Thermo Scientific). Meanwhile, electrochemical performance analysis of the CS/rGO/CuO-modified SPE electrode for urea detection was performed using cyclic voltammetry (CV) with a CorrTest Electrochemical Workstation type. This method involved the configuration of a three-electrode system, including a reference electrode (Ag/AgCl), an auxiliary electrode (Pt) and a working electrode. The optimum scan rate and modified electrode were further applied to the next step. All procedures are illustrated in Fig. 1 (Fig. S1).

3. Results and discussion

3.1 FTIR analysis

A FTIR study of CS, CS/rGO, and CS/rGO/CuO films, which were obtained from the electrodeposition technique, was performed to compare the characteristics of functional groups between chitosan as a matrix film and the chitosan, which was modified with rGO and CuO, as displayed in Fig. 2 (Fig. S2). It was examined using a spectrometer manufactured by Shimadzu IR Prestige 21 in the range of 4000–450 cm⁻¹ spectral region. In terms of the FTIR functional groups of CS, the peak at 3245.18 cm⁻¹ represents the stretching of hydroxyl groups. The peak at 2875.09 cm⁻¹ indicates the stretching vibration of the C-H saturated aliphatic. C=O stretching contributes to the peak of 1628.11 cm⁻¹, while the primary amine (N-H) stretching is assigned at 1464.71 cm⁻¹. The peak of 1064.0 cm⁻¹ is associated with the C–O–C asymmetric stretching vibration bonds of CS.^{28,31} Meanwhile, the FTIR spectrum of the film

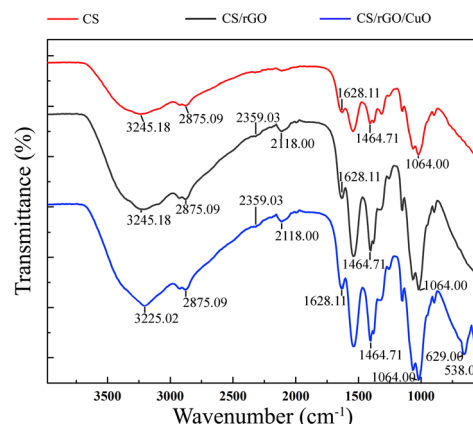


Fig. 2 FTIR spectra of CS, CS/rGO, and CS/rGO/CuO films.

based on CS/rGO shows regular peaks assigned to CS (3245.18 cm⁻¹, 2875.09 cm⁻¹, 1628.11 cm⁻¹, 1464.71 cm⁻¹, and 1064 cm⁻¹), presenting similar peaks.³¹ In contrast, the absorption peak intensities declined slightly on CS/rGO. This was influenced by the addition of rGO. This also indicates that rGO was distributed into the CS film; it is likely inferred that only physical interaction occurs on the composite, such as a hydrogen bond. Additionally, the FTIR spectra of the CS/rGO/CuO film indicated that the absorption peak differed from that of the previous films. Furthermore, the incorporation of CuO into the CS/rGO film was confirmed through FTIR spectra. The spectrum shows the appearance of absorption bands at 629.0 cm⁻¹ and 538 cm⁻¹. These bands indicate the presence of typical Cu–O group vibrations, confirming the successful synthesis of the CS/rGO/CuO composite film.³² The spectra correspond to the oscillations produced by the Cu–O bond. The existence of the Cu–O bond indicates the successful incorporation of CuO to the amine group, indicating the successful synthesis of CS/rGO/CuO film. Similarly, the mixing process of rGO and CuO into the CS matrix film was successful, exhibiting a homogeneous solution. This also indicated that rGO and CuO were well distributed. Therefore, the CS/rGO/CuO-based composite can be applied to the working electrode's sensitive layer to detect urea fertilizer. Several analyses were performed to ensure a successful process.

3.2 XRD analysis

The XRD diffractogram of the CS film is shown in Fig. 3a (Fig. S3). This diffractogram shows two main diffraction peaks at $2\theta = 10^\circ$ and 20° , which correspond to the ordered polymer chain structure and semi-crystalline nature of CS, respectively. No other peaks were found, indicating the presence of impurities in the pure CS film. After the incorporation of rGO into the CS matrix (Fig. 3b and S3), no significant changes were found to the diffraction pattern compared to the diffraction pattern of pure CS. The CS/rGO composite still shows peaks at $2\theta = 10^\circ$ and 20° , which indicates that the nanocomposite still maintains its crystallinity. A new peak appears around $2\theta = 25$ – 26° . These peaks are identical to the characteristic peaks of rGO,

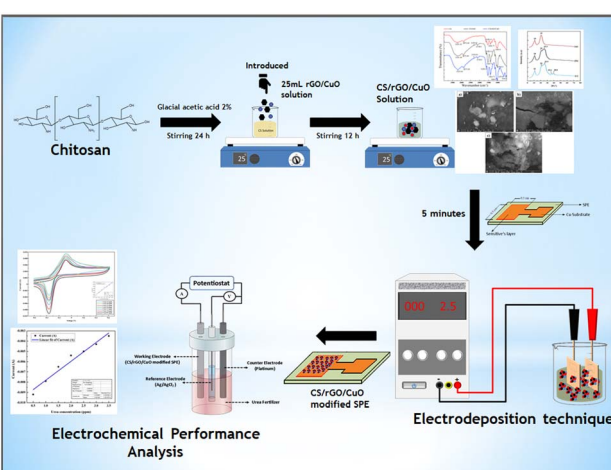


Fig. 1 Schematic of urea fertilizer detection using CS/rGO/CuO-modified SPE.



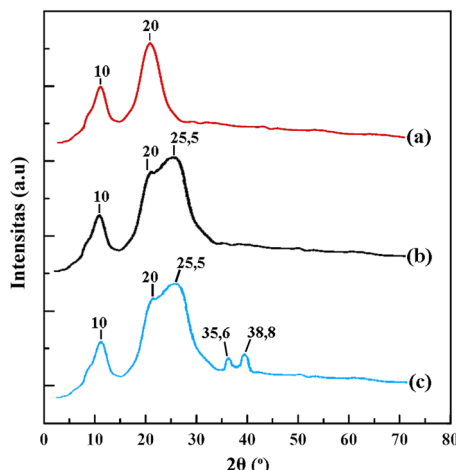


Fig. 3 XRD diffractograms of CS (a), CS/rGO (b) and CS/rGO/CuO (c).

indicating that rGO is successfully dispersed in the chitosan matrix and forms a new composite structure.²⁸

Additionally, Fig. 3c (Fig. S3) presents the XRD diffractogram of CS/rGO/CuO. After the addition of CuO, two new diffraction peaks appear at $2\theta = 35.6^\circ$ and 38.8° , which correspond to the typical diffraction pattern of CuO based on the literature.³² The appearance of these peaks confirms that CuO remains in crystalline form after incorporation into the composite. Furthermore, the loading process of rGO and CuO within the CS matrix can be proven through FE-SEM analysis.

3.3 FE-SEM analysis

The surface morphologies of CS, CS/rGO, and CS/rGO/CuO films are studied utilising FE-SEM with 20 kV accelerated voltage. Fig. 4 (Fig. S4) presents 50 000 \times magnification FE-SEM micrographs of CS, CS/rGO, and CS/rGO/CuO, highlighting notable variations. The images of FE-SEM (Fig. 4a) show that the surface of the CS film appears relatively smooth with little roughness, with no noticeable gaps. This structure indicates that the CS film has good compaction, which makes it suitable as a matrix for sensor applications. However, the CS/rGO film

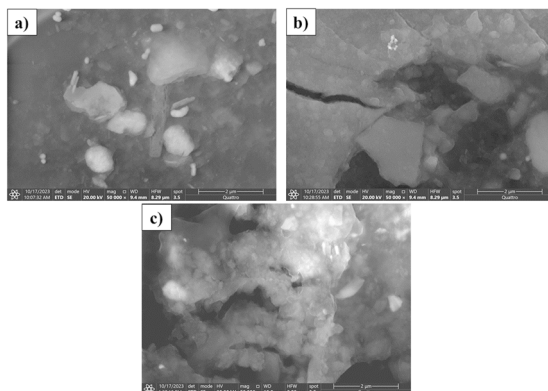


Fig. 4 FE-SEM images of CS (a), CS/rGO (b) and CS/rGO/CuO (c).

depicted in Fig. 4b exhibits a uniform dispersion of rGO nanoparticles within the CS film. This is due to the homogeneous mixing process between CS and rGO.^{32,33} Conversely, the incorporation of rGO and CuO into the CS film led to a modification in the CS film structure, resulting in agglomeration (Fig. 4c). The homogeneously dispersed rGO/CuO and the presence of agglomeration indicate a strong interaction of the three components, indicating that CuO and rGO are attached to the surface and physically bonded with chitosan.

However, it is believed that agglomeration does not significantly affect its potential as a sensitive material for detecting urea fertilizer. To demonstrate this, a comprehensive analysis of its electrochemical characteristics is conducted using cyclic voltammetry (CV).

3.4 Electrochemical performance analysis

3.4.1 Cyclic voltammetry measurement of the chitosan-modified SPE vs. chitosan/rGO/CuO-modified SPE. The electrochemical performance of both modified electrodes is evaluated in a PBS solution with a pH of 7. The scanning potential is used from -0.6 V to $+0.6$ V, with a scan rate of 100 mV s $^{-1}$. Both modified electrodes displayed a pair of redox peaks, anodic and cathodic, as the interaction of the working electrode with ions in PBS as well as the effect of solution pH on the electrode surface. The presence of CuO on the working electrode, which is known to be pH-sensitive, can cause a potential shift and the appearance of redox peaks due to electrode surface reaction.

However, the intensities and potentials of these peaks differ between these two modified electrodes. The electrochemical response of the CS/rGO/CuO-modified electrode was better than the CS-based electrode, as shown in Fig. 5 (Fig. S5). Furthermore, the modified electrode based on CS/rGO/CuO resulted in the anodic peak current (I_{pa}) and cathodic peak current (I_{pc}), as shown in Table 1.

It is observable that the reactivity and electrical properties of the produced modified electrode can be observed when it reacts in PBS solution, as shown in (eqn (1)–(3)). In PBS electrolyte

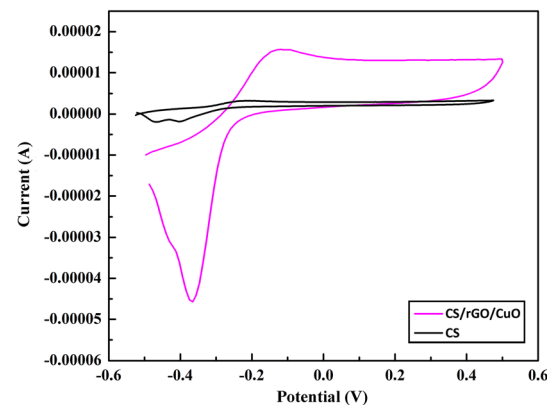


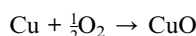
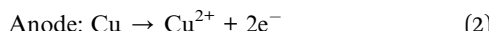
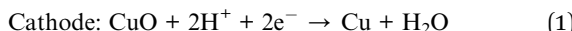
Fig. 5 CV voltammograms of electrodes modified with CS/rGO/CuO and CS and then dipped in a PBS solution with a pH of 7 at a scan rate of 100 mV s $^{-1}$.



Table 1 Electrochemical performance data of CS-modified electrode vs. CS/rGO/CuO-modified electrode using cyclic voltammetry

Electrode	I_{pa} (A)	I_{pc} (A)	E_{pa} (V)	E_{pc} (V)	ΔE_p (V)
CS	2.1×10^{-6}	-9.3×10^{-6}	-0.22	-0.40	0.15
CS/rGO/CuO	1.53×10^{-5}	-4.56×10^{-5}	-0.13	-0.37	0.27

solution (pH 7), CuO undergoes a stepwise reduction process of $\text{Cu}^{2+} \rightarrow \text{Cu}^+ \rightarrow \text{Cu}$, resulting in two separate reduction peaks on the CV plot at a given potential. Variations in the potential values of the redox peaks indicate that the mechanism depends on the interactions among CuO, the electrode, and the solution.



Interaction of CuO with PBS solution



The most crucial factor to consider in the electrochemical analysis of redox reactions employing cyclic voltammetry (CV) is the scan rate. Therefore, the impact of scan rate on the voltammetric outcomes of the modified electrode was assessed by measuring the CV in PBS solution with a pH of 7.

3.4.2 Scan rate study. The optimal scan rate was determined by observing the effect of the exchange's electron flow. Briefly, it was conducted on a modified electrode utilising the CV approach in PBS solution (pH 7) and the obtained I_{pa} and I_{pc} (Fig. 6 and S6). In this study, the recorded potential range was from -0.6 to +0.6 V, with scan rates of 25 mV s⁻¹, 50 mV s⁻¹, 75 mV s⁻¹, and 100 mV s⁻¹. These scan rate ranges were utilised to prevent the occurrence of small current peaks and peak overlap, which could compromise the selectivity of the analysis.

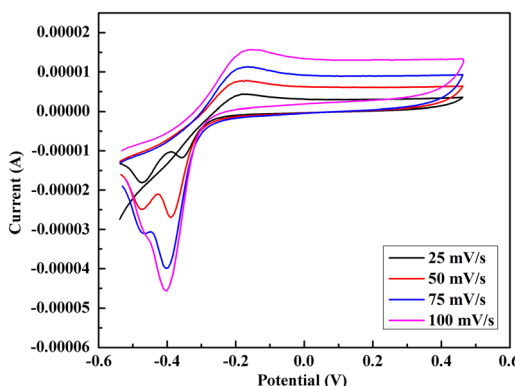


Fig. 6 Cyclic voltammograms at different scan rates for the CS/rGO/CuO-modified SPE electrode.

This was achieved by avoiding the use of too large scan rate values. Moreover, a more rapid scan rate can inflict damage on the electrode owing to the swift change in electrical potential. Conversely, a slower scan rate is not well-suited for examining rapid kinetic phenomena.³⁴

Furthermore, the I_{pa} and I_{pc} test results of the modified electrode, which were set within scan rates of 25, 50, 75, and 100 mV s⁻¹, are shown in Table 2. Table 2 illustrates that the optimal scan rate is observed at 100 mV s⁻¹, with I_{pa} and I_{pc} values of 1.53×10^{-5} and -4.56×10^{-5} , respectively. Nainggolan *et al.* (2024) also reported that the optimal scan rate that can be used is 100 mV s⁻¹.³⁰ However, I_{pa} and I_{pc} peak currents present linear response dependence upon the square root of the scan rate. The R^2 value for I_{pa} and I_{pc} were calculated to be 0.9844 and 0.9817, respectively, as shown in (Fig. 7 and S7). When these values become closer to 1, it indicates that the redox mechanism in the CS/rGO/CuO system may involve two simultaneous contributions: (1) diffusive transport of species in PBS solution and (2) charge transfer *via* CuO species adsorbed on the electrode. This mechanism is consistent with previous studies of CuO-based systems on working electrodes.^{35,36}

3.4.3 Measurement of optimal modified electrode in phosphate buffer saline solution. Fig. 8 (Fig. S8) indicates the I_{pc} of the modified electrode by various concentrations of CuO in PBS solution (pH 7) with potential ranging from -0.6 V to +0.6 V at a scan rate of 100 mV s⁻¹. This step was conducted to obtain the best concentration of CuO; then, it was applied to detect the urea concentration. The peak current of each modified electrode, which was added by various concentrations of CuO, is displayed in Table 3.

Fig. 8 (Fig. S8) and Table 3 show that the addition of different CuO concentrations gives different peak currents. Of all the SPE electrodes modified with CS/rGO/CuO, the addition of 8% (g L⁻¹) of CuO to the modified electrode resulted in a maximum peak reduction current (I_{pc}) of -4.56×10^{-5} A. This is due to the increased number of electrochemically active centres on the electrode surface, which enhances electron transfer and strengthens the voltammetric response. However, at higher CuO concentrations, agglomeration may reduce the effectiveness of the active areas, leading to changes in the redox current. Therefore, the optimal CuO content needs to be determined to achieve maximum sensitivity. Magar *et al.* (2023) reported that the electrode with the optimum CuO concentration showed increased electrochemical activity and charge transfer efficiency, indicating effective catalysis of urea oxidation as well as high sensitivity to urea detection without additional measurements.³⁷

Table 2 I_{pa} and I_{pc} values for determining optimal scan rates

Scan rate (mV s ⁻¹)	I_{pa} (A)	I_{pc} (A)
25	4.1×10^{-6}	-1.1×10^{-5}
50	7.6×10^{-6}	-2.7×10^{-5}
75	1.2×10^{-5}	-4.0×10^{-5}
100	1.53×10^{-5}	-4.56×10^{-5}



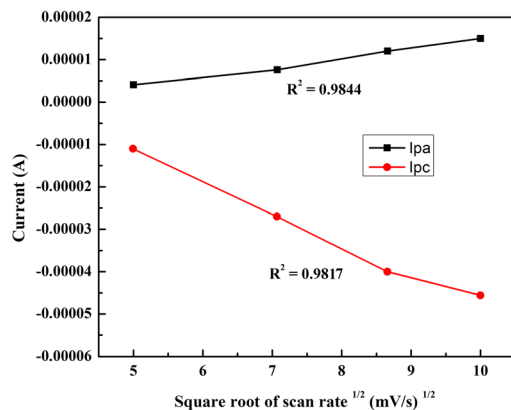


Fig. 7 The effect of scan rate on the anodic (and cathodic) peak current is presented, with the inset showing a linear fit of peak current versus the square root of the scan rate, indicating a diffusion-controlled process.

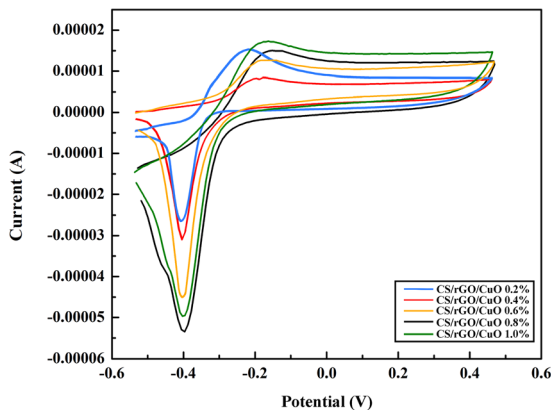


Fig. 8 CV voltammograms of the modified electrode based on CS/rGO/CuO with different concentrations of CuO.

Table 3 Peak current of the modified electrodes

CuO (%)	I_{pa} (A)	I_{pc} (A)	E_{pa} (V)	E_{pc} (V)	I_{pc}/I_{pa}	ΔE_p (V)
0.2	1.55×10^{-5}	-2.6×10^{-5}	-0.22	-0.41	-1.67	0.19
0.4	1.70×10^{-5}	-3.1×10^{-5}	-0.17	-0.40	-4.42	0.23
0.6	1.25×10^{-5}	-3.6×10^{-5}	-0.13	-0.40	-2.88	0.27
0.8	1.53×10^{-5}	-4.56×10^{-5}	-0.17	-0.40	-2.98	0.23
1.0	1.5×10^{-5}	-4.5×10^{-5}	-0.18	-0.40	-3.00	0.22

Meanwhile, the linearity result of the R -square (R^2) obtained from the modified electrode is 0.9361. Based on the previous study reported by ref. 38, the excess CuO concentration in the modified electrode can cause the electrode surface to be too thick, hindering electron transfer and ion diffusion. In addition, it can cause excessive reactivity and physical and chemical changes of the modified electrode, such as the release of CuO particles into the solution, to interfere with the main reaction and cause instability and contamination of the electrolyte solution. On the contrary, a lack of CuO concentration may decrease catalytic activity, electron transfer efficiency, and

sensitivity. Therefore, an appropriate CuO concentration is the focus of this study to ensure good electrode efficiency, sensitivity, and stability. Therefore, a modified electrode based on CS/rGO/CuO 0.8% was further used to detect urea fertilizer.

3.4.4 Electrochemical study of urea. To confirm the role of each material component, electrochemical studies of urea were carried out using CS/rGO and CS/CuO-modified SPE electrodes, as shown in Fig. 9 (Fig. S9). Fig. 9a shows the CV voltammogram of CS/rGO-modified SPE in the presence of various concentrations of urea fertilizer at a scan rate of 100 mV s^{-1} . The selected rGO concentration was $250 \mu\text{M}$. The selection of this concentration refers to the research conducted by Sembiring *et al.* 2023,²⁸ which stated that the optimum concentration of rGO on the CS/rGO electrode is a sensing material. In addition, Nainggolan *et al.* (2024) also reported that an rGO concentration of 250 ppm was chosen for further analysis of cholesterol using a modified CS/rGO/MnO₂ electrode.³⁰ From the CV voltammogram of urea using the CS/rGO-modified SPE electrode, the LoD and LoQ values were $7.26 \mu\text{M}$ and $24.22 \mu\text{M}$, respectively. In this case, rGO plays a role in enhancing the conductivity and electron transfer of the CS/rGO-modified SPE electrode, but rGO does not have many active sites for urea catalysis during the electrochemical process. Consequently, although this electrode has high conductivity, its catalytic ability in detecting urea was limited. Meanwhile, on the CS/CuO-modified SPE electrode, CuO has catalytic properties towards the urea oxidation reaction. In the CS/CuO electrode, CuO acts as an active site to increase the rate of the urea redox reaction. However, compared to rGO, CuO has lower conductivity, which may limit the charge transfer efficiency in the electrode. Furthermore, despite its better catalytic activity, the lack of materials with high conductivity in this electrode may lead to higher resistance compared to CS/rGO, so the electrochemical response may not be as good as expected. This can be observed from the CV voltammogram of the CS/CuO-modified SPE electrode, as shown in Fig. 9b. As depicted in Fig. 9b, the LoD and LoQ values obtained are $3.04 \mu\text{M}$ and $12.01 \mu\text{M}$, respectively. It can be concluded that the addition of rGO into the CS film plays a role in increasing electron transfer, but it has a lower peak current. On the contrary, the addition of CuO into the CS electrode can increase the catalytic activity of the electrode, which is indicated by a higher peak current. Therefore, combining rGO and CuO into CS film makes the CS/rGO/CuO-modified SPE electrode an optimal strategy to utilize the advantages, *i.e.* enhancing

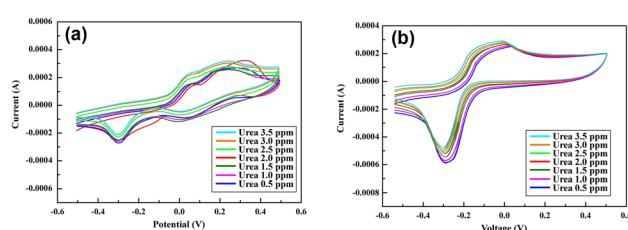


Fig. 9 CV voltammograms of CS/rGO-modified SPE (a) and CS/CuO-modified SPE electrode (b) in the presence of various concentrations of urea fertilizer at a scan rate of 100 mV s^{-1} .

electron transfer and providing sufficient catalytically active sites for more sensitive urea detection.

Considering the CV voltammogram acquired *via* various modified electrodes, the CS/rGO/CuO-modified SPE electrode exhibits significantly more prominent oxidation and reduction peaks compared to the CS, CS/rGO, and CS/CuO-modified SPE electrodes (Fig. 10). The findings clearly show the enhanced electrochemical activity of CS/rGO/CuO-modified SPE owing to their higher surface area. Next, the CV approach was used to evaluate the electrochemical study of urea fertilizer sensing, followed by its mechanism. During the electrochemical process of urea fertilizer, the produced I_{pa} and I_{pc} values are presented in Table 4. However, Fig. 10 (Fig. S10) illustrates a decrease in cathodic current with increasing urea concentration, suggesting that the reduction reaction does not proceed with the same efficiency as oxidation. This could be due to the adsorption of oxidation products, such as CO_2 , on the electrode, which inhibits the reduction process, as has been reported in the literature.³⁹ Since CuO on the electrode acts as a catalyst, the competition of electrochemical reactions on the electrode may also cause an imbalance in the redox current. Thus, although the oxidative current increased proportionally with urea concentration, the cathodic current showed a different trend, indicating the more complex nature of the reaction kinetics.

Table 4 demonstrates that CV measurements reveal distinct current peaks, which are caused by the oxidation process of urea. An increase in the concentration of urea in the solution leads to a corresponding increase in the peak oxidation current, which demonstrates the electrode's sensitivity to urea. The reduction process can occur when the products generated in the oxidation process can interact with the electrode again. Thus, it is clear that the CS/rGO/CuO-modified SPE has remarkable electrocatalytic performance at the interface. The schematic representation of the reaction mechanism of urea fertilizer detection using CS/rGO/CuO modified SPE is shown in Fig. 11 (Fig. S11).

The linearity and sensitivity determination of CS/rGO/CuO modified SPE is calculated using the least square method as

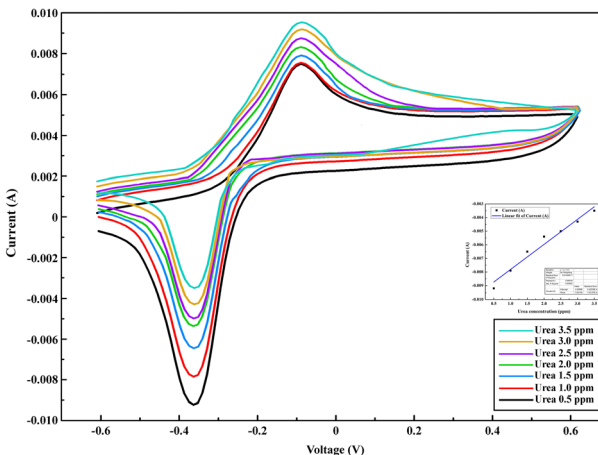


Fig. 10 CV voltammograms of CS/rGO/CuO-modified SPE in the presence of various concentrations of urea fertilizer at a scan rate of 100 mV s^{-1} .

Table 4 I_{pa} and I_{pc} values for detecting urea fertilizer

Urea (ppm)	I_{pa} (A)	I_{pc} (A)	I_{pc}/I_{pa}	R-Square
0.5	0.0062	-0.0092	-1.4838	0.9599
1.0	0.0076	-0.0079	-1.0394	
1.5	0.0079	-0.0065	-0.8227	
2.0	0.0083	-0.0054	-0.6506	
2.5	0.0088	-0.0050	-0.5681	
3.0	0.0092	-0.0043	-0.4673	
3.5	0.0096	-0.0035	-0.3645	

given in eqn (4), where y is a dependent variable while a , b , and x are slope, intercept, and urea concentration, respectively.

$$y = a + bx \quad (4)$$

Based on the least squares method used, the R -square (R^2) value from the linear calibration curve was 0.9599, which showed a diffusion-controlled process, as shown in Fig. 10. Additionally, the sensitivity's modified electrode was calculated to be $-1.9 \times 10^{-5} \mu\text{A} \mu\text{M}^{-1}$. In addition, LoD and LoQ determinations were conducted in this study. LoD determination was conducted to ascertain the minimum detectable concentration of the analyte solution that could be detected by the working electrode. However, LoQ determination was carried out to determine the least detectable concentration value based on its capacity to measure the least concentration of an analyte. The LoD and LoQ calculations were performed based on the standard deviation (SD) of the blank signal and the slope of the calibration curve, as proposed in the analytical literature.³¹ The low LoD value indicates the high sensitivity of the developed sensor. In this study, the SD intercept and slope values obtained are 4.47×10^{-3} and 1.84×10^{-3} , respectively. Therefore, the values for LoD and LoQ values were further calculated utilizing eqn (5) and (6):

$$\text{LoD} = \frac{3 \times \text{SD intercept}}{\text{Slope}}, \quad (5)$$

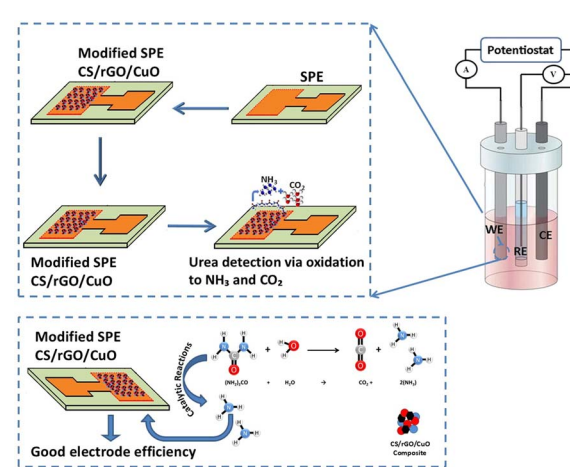


Fig. 11 Schematic of the reaction mechanism of urea fertilizer detection using CS/rGO/CuO-modified SPE.³⁶

$$\text{LoQ} = \frac{10 \times \text{SD intercept}}{\text{Slope}}. \quad (6)$$

Based on the calculation above, LoD and LoQ are found to be 0.14 μM and 0.49 μM , respectively. This proves that the CS/rGO/CuO-modified electrode has excellent potential to be utilized as a working electrode for detecting urea fertilizer concentrations. In addition, these data are evidence that CS/rGO/CuO-modified SPE can work at the minimum detectable concentration compared to previous work, as reported. A comparison of the electrochemical performance of various working electrode-based modified SPEs in detecting urea is shown in Table 5.

3.4.5 Interference, reproducibility, and lifetime of the CS/rGO/CuO-modified SPE electrode. An interference study of the CS/rGO/CuO-modified SPE electrode was proposed to evaluate the reliability of the sample measurements. In this study, several interfering substances, such as Na^+ , PO_4^{3-} , NO_3^- , and K^+ , were added into a 1 μM urea solution diluted with PBS solution ($\text{pH} = 7$). Urea solution was used as a positive control. In the process, a 5-fold excess of the interfering substances was added into the urea solution, and their electrochemical responses were tested using CV. The results of the interference study are shown in Fig. 12 (Fig. S12). As depicted in Fig. 12, the bar graph shows that the addition of interfering substances into the urea solution resulted in a slight decrease in the peak current. However, this decrease in the peak current did not show significant changes in the position and peak current. Therefore, the fabricated CS/rGO/CuO-modified SPE electrode shows high sensitivity and selectivity for urea detection.

A reproducibility study was carried out to determine the electrochemical performance of the CS/rGO/CuO-modified SPE electrode because it can be used as an indicator of the accuracy of the working electrode when the measurement results are consistent under the same conditions. In this study, the reproducibility of the CS/rGO/CuO-modified SPE electrode was tested using seven electrodes to detect urea concentration (1 ppm), as displayed in Fig. 13 (Fig. S13). The measurement results showed that the current obtained ranged from $-0.0075 \mu\text{A}$ to $0.0079 \mu\text{A}$, with an average (\bar{X}) of $-0.00767 \mu\text{A}$ and a standard deviation (SD) of $0.00020 \mu\text{A}$. Thus, the Relative Standard Deviation (RSD) value obtained is 2.70%, indicating that the produced electrode has high reproducibility and can be

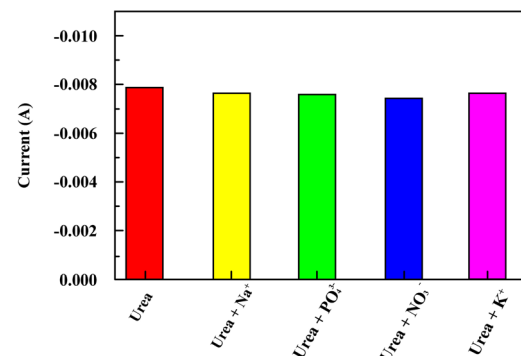


Fig. 12 Interference bar graph of the CS/rGO/CuO-modified SPE electrode.

used for urea analysis consistently. The RSD was calculated using the following equation:

$$\% \text{RSD} = \frac{\text{SD}}{\bar{X}} \times 100\%. \quad (7)$$

Furthermore, a lifetime study of the CS/rGO/CuO-modified SPE electrode was conducted to determine the consistency of the results provided over a period of time without experiencing significant degradation. The electrodes were tested for 5 weeks by taking measurements every 7 days in a 1.0 μM urea solution using the CV method. The electrodes were stored at 25 $^\circ\text{C}$ under dry conditions when not in use, and the current response was analyzed to assess performance degradation. The CV voltammogram of the lifetime study of the CS/rGO/CuO-modified SPE electrode is presented in Fig. 14 (Fig. S14).

As illustrated in Fig. 14, it can be observed that the measurement result shows that the current of the CS/rGO/CuO-modified SPE electrode only decreased by 1.98% in the first three weeks. Meanwhile, the decreasing currents in the 4th and 5th weeks were 2.24% and 2.52%, respectively. This value indicates that the resulting electrode can still be used effectively for up to 5 weeks before experiencing significant degradation. In addition, it showed better stability because the CS/rGO/CuO combination can improve the durability of the CS/rGO/CuO-modified SPE electrode through enhanced adhesion and electrochemical stability.

Table 5 Comparison of the electrochemical performance of various working electrodes in detecting urea

Electrode material	Method	LoD (μM)	LoQ (μM)	Sensitivity ($\mu\text{A } \mu\text{M}^{-1} \text{ cm}^{-2}$)	Ref.
NiO nanostructure-modified GCE	CV	20	90	—	40
MnO ₂ /rGO-modified platinum	CV	14.693	—	9.7×10^{-3}	36
ZnO nanostructure-modified graphite electrode	CV	2.5	—	—	41
MoS ₂ QDs	Ratiometric fluorescence	1.8	—	—	42
Ti/RuO ₂ -TiO ₂ -SnO	CV/LSV	1.83	7.66	9205	
ZSs@rGO	CV	0.012	—	682.8	43
CS/rGO/CuO	CV	0.14	0.49	1.93×10^{-3}	Present work



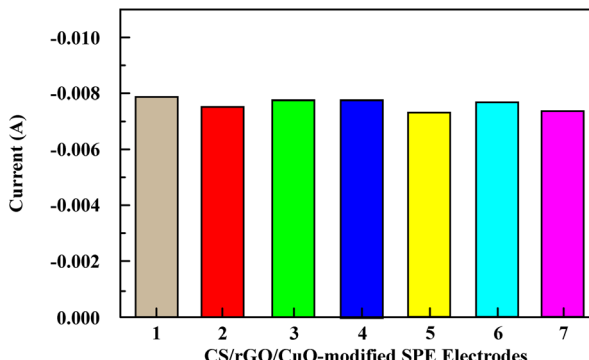


Fig. 13 Reproducibility bar graph of the CS/rGO/CuO-modified SPE electrode.

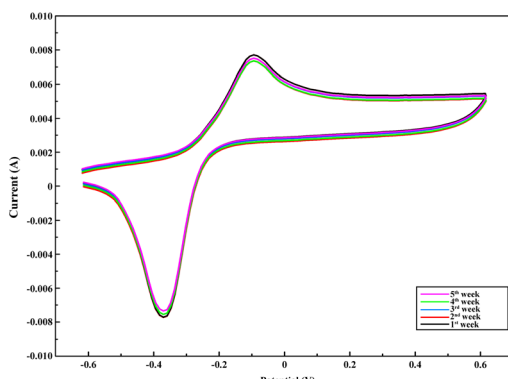


Fig. 14 CV voltammograms of the lifetime study of the CS/rGO/CuO-modified SPE electrode.

3.4.6 Determination of urea in real samples. The detection of urea in real samples, such as tap water and field water, is essential to evaluate the effectiveness of the CS/rGO/CuO-modified SPE electrodes under complex environmental conditions. The presence of other ions in water can affect the electrochemical performance of the electrode, so it is necessary to test real samples to ensure the selectivity and reliability of the method used. In this study, the urea solution in PBS (pH = 7) was used as a positive control. Next, real samples (tap water and field water) were added with 0.5 μ M urea solution. The CV voltammogram of urea determination in real samples is displayed in Fig. 15 (Fig. S15), where it was calculated based on the recovery test. Furthermore, the resulting I_{pa} and I_{pc} values of the urea fertilizer detection in real samples are presented in Table 6 (Reviewer#1, Comment#1).

Urea fertilizer concentration in field water and tap water can be determined using I_{pa} and I_{pc} values, as shown in Table 6. Then, the concentration values were calculated using eqn (8), which employs the linear calibration equation. In addition, the recovery values (%) were determined using eqn (9). This approach uses the ratio between the peak currents (I_{pc}), predicated on the assumption that^{44–46}

$$\frac{C_{\text{sample}}}{C_{\text{standard}}} = \frac{I_{pc \text{ sample}}}{I_{pc \text{ standard}}}, \quad (8)$$

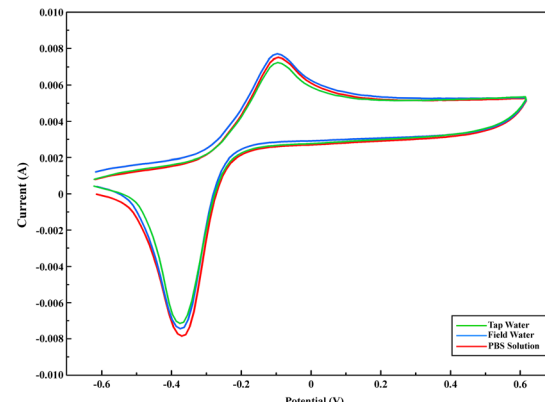


Fig. 15 CV voltammograms of urea determination in real samples using the CS/rGO/CuO-modified SPE electrode.

Table 6 I_{pa} and I_{pc} values for detecting urea fertilizer in real samples

Real sample	I_{pa} (A)	I_{pc} (A)	I_{pc}/I_{pa}	Recovery (%)
PBS	0.00785	-0.00792	-1.008917	100
Field water	0.00776	-0.00788	-1.015464	99.49
Tap water	0.00754	-0.00766	-1.015915	96.71

$$\text{Recovery}(\%) = \frac{C_{\text{detected}}}{C_{\text{added}}} \times 100\%. \quad (9)$$

The detected concentrations of urea in both field water and tap water samples were found to be lower than the standard concentration (0.5 μ M) prepared in phosphate buffer solution (PBS). Specifically, the detected urea concentrations were 0.4974 μ M in field water and 0.4802 μ M in tap water, corresponding to recovery values of 99.49% and 96.71%, respectively. The reduction in the observed urea concentration results from matrix effects in real samples. In contrast to purified and controlled PBS, field water and tap water contain contaminants, such as organic matter, metal ions, or fertilizer residues. These chemicals may compete with urea on the electrode surface, alter the electrochemical conditions, or induce fouling, thereby diminishing sensor sensitivity. Moreover, variations in conductivity and buffer capacity relative to PBS may disrupt electron transfer efficiency, resulting in a slight underestimation of urea concentration measurement outcomes. These results show that the proposed CS/rGO/CuO-modified SPE electrode can directly detect urea in real samples. The recovery values for field water and tap water samples were 99.49% and 96.71%, respectively, which indicates that the CS/rGO/CuO-modified SPE electrode performed reliably in complicated matrices, adhering to typical validation criteria that deem 90–100% recovery considered acceptable for real sample analysis.^{44,45}

4. Conclusions

This study presents a new strategy by developing a novel sensitive working electrode based on a screen-printed electrode, which is modified with CS/rGO/CuO for detecting urea concentration. The



prepared CS/rGO/CuO was effectively studied using FTIR, XRD, and FE-SEM. The characterization results showed that the material combination used was able to increase the electrode surface area and accelerate electron transfer, greatly contributing to electrochemical performance. Moreover, the CS/rGO/CuO modified SPE is electrochemically tested using CV. The addition of CuO is shown to impact the properties of CS/rGO/CuO-modified SPE. From the results of this study, it is known that CS/rGO/CuO modified SPE with added CuO results in an increase in the electrochemical activity of the modified SPE. The optimal concentration of CuO found to be added to CS/rGO/CuO is 0.8%, resulting in an I_{pc} value of -4.56×10^{-5} . Further studies on R^2 determination of the modified electrode also showed good performance at 0.9361, indicating its reaction's electron transfer is under diffusion control. Thus, this condition makes the CS/rGO/CuO-modified SPE, as a working electrode, a highly cost-effective tool for urea fertilizer analysis at various concentrations. Furthermore, in the case of urea fertilizer detection, it can be observed that CS/rGO/CuO-modified SPE presented good electrochemical performance R^2 of 0.9599 and showed excellent sensitivity of 1.9×10^{-3} ($\mu\text{A } \mu\text{M}^{-1} \text{ cm}^{-2}$). However, the SPE's modification can sense urea at both higher and lower concentrations, with LoD and LoQ values of 0.14 μM and 0.49 μM , respectively. Thus, the CS/rGO/CuO modified SPE is equally suitable for detecting urea fertilizer.

Author contributions

Irwana Nainggolan: writing – review & editing, writing – original draft, validation, supervision, investigation, funding acquisition, conceptualization. Ardiansyah Sembiring: writing – original draft, methodology, investigation, formal analysis, data curation, conceptualization. Tulus Ikhsan Nasution: writing – review & editing, visualization, supervision. Rahmadhani Banurea: writing – review & editing. Reka Mustika Sari: writing – review & editing, formal analysis, data curation. Andriyani: writing – review & editing, supervision. Rozyanty Rahman: writing – review & editing. Bing Li: writing – review & editing. Rica Asrosa: writing – review & editing. Khatarina Meldawati Pasaribu: data curation, writing – review & editing.

Conflicts of interest

The authors state that they do not have any conflicts of interest.

Data availability

Additional datasets generated and analyzed during this study are available from the corresponding author upon reasonable request.

All data supporting this study are provided in the main article and SI. See DOI: <https://doi.org/10.1039/d4ra08451a>.

Acknowledgements

The authors acknowledge the funding provided by PTUPT scheme from the Ministry of Education, Culture, Research, and

Technology, RI with a contract number 84/UN5.2.3.1/PPM/KP-DRTPM/L/2022. Authors also thank the Center of Excellent Chitosan and Advance Materials and postgraduate school of chemistry laboratory, Universitas Sumatera Utara for providing the facilities to conduct the research and characterisation.

References

- D. Shanmugavel, I. Rusyn, O. Solorza-Feria and S. K. Kamaraj, Sustainable SMART fertilizers in agriculture systems: A review on fundamentals to in-field applications, *Sci. Total Environ.*, 2023, **904**, 166729, DOI: [10.1016/j.scitotenv.2023.166729](https://doi.org/10.1016/j.scitotenv.2023.166729).
- P. Krasilnikov, M. A. Taboada and A. Amanullah, Fertilizer Use, Soil Health and Agricultural Sustainability, *Agriculture*, 2022, **12**(4), 16–20, DOI: [10.3390/agriculture12040462](https://doi.org/10.3390/agriculture12040462).
- FAO, Fertilizer use by crop in Indonesia, *Trop. Agric.*, 2005, **47**, 7.
- S. Swify, R. Mažeika, J. Baltrusaitis, J. Drapanauskaitė and K. Barčauskaitė, Review: Modified Urea Fertilizers and Their Effects on Improving Nitrogen Use Efficiency (NUE), *Sustainability*, 2023, **16**, 1–20.
- C. R. S. A. Filho, A. L. R. M. Rossete, C. R. O. Tavares, C. V. Prestes and J. A. Bendassolli, Synthesis of 15 N-Enriched Urea (Co(15 Nh 2)2) From 15 Nh 3, Co, and S in a Discontinuous Process, *Braz. J. Chem. Eng.*, 2012, **29**, 795–806.
- Balitbangtan, Pupuk Kimia Memiliki Kekurangan dan Kelebihan, Kementerian Pertanian Badan Litbang Pertanian, 2019, <http://www.litbang.pertanian.go.id/tahukah-anda/223/>.
- M. Fernández-Delgado, E. del Amo-Mateos, S. Lucas, M. T. García-Cubero and M. Coca, Liquid fertilizer production from organic waste by conventional and microwave-assisted extraction technologies: Techno-economic and environmental assessment, *Sci. Total Environ.*, 2022, **806**(4), 150904, DOI: [10.1016/j.scitotenv.2021.150904](https://doi.org/10.1016/j.scitotenv.2021.150904).
- P. Ri, Pupuk Organik, Pupuk Hayati Dan Pemberah Tanah, Peraturan Menteri Pertanian, 2011, vol. **70**, pp. 1–109, <https://psp.pertanian.go.id/storage/545/Permentan-No.-70-Th.-2011-ttg-Pupuk-Organik-Pupuk-Hayati-dan-Pemberah-Tanah.pdf>.
- M. A. Ali, L. Dong, J. Dhau, A. Khosla and A. Kaushik, Perspective—Electrochemical Sensors for Soil Quality Assessment, *J. Electrochem. Soc.*, 2020, **167**, 037550.
- R. Gunawan, T. Andhika. S. and F. Hibatulloh, Monitoring System for Soil Moisture, Temperature, pH and Automatic Watering of Tomato Plants Based on Internet of Things, *Telekontran*, 2019, **7**(1), 66–78, DOI: [10.34010/telekontran.v7i1.1640](https://doi.org/10.34010/telekontran.v7i1.1640).
- M. I. Hossain, M. A. Khaleque, M. R. Ali, M. S. Bacchu, M. S. Hossain, S. M. F. Shahed, M. Saad Aly and Z. H. Khan Md., Development of electrochemical sensors for quick detection of environmental (soil and water) NPK ions, *RSC Adv.*, 2024, **14**(13), 9137–9158, DOI: [10.1039/D4RA00034J](https://doi.org/10.1039/D4RA00034J).

12 L. Quadrini, S. Laschi, C. Ciccone, F. Catelani and I. Palchetti, Electrochemical methods for the determination of urea: Current trends and future perspective, *TrAC, Trends Anal. Chem.*, 2023, **168**, 117345.

13 P. Batista Deroco, J. d. F. Giarola, D. Wachholz Júnior, G. Arantes Lorga and L. Tatsuo Kubota, Paper-Based Electrochemical Sensing Devices, *Comprehensive Analytical Chemistry*, Elsevier B.V., 2020, vol. 89, pp. 91–137, DOI: [10.1016/bs.coac.2019.11.001](https://doi.org/10.1016/bs.coac.2019.11.001).

14 V. Periasamy, P. N. N. Elumalay, S. Talebi, R. T. Subramaniam, R. Kasi, M. Iwamoto and G. Gnana kumar, Novel same-metal three electrode system for cyclic voltammetry studies, *RSC Adv.*, 2023, **13**, 5744–5752, DOI: [10.1039/D3RA00457K](https://doi.org/10.1039/D3RA00457K).

15 Y. Gao, Y. Guo, P. He, Z. Liu and Y. Chen, Enhanced sensitivity and selectivity of an electrochemical sensor for real-time propofol monitoring in anesthesia, *Alexandria Eng. J.*, 2024, **87**, 47–55.

16 W. Raza and K. Ahmad, A highly selective Fe @ ZnO modified disposable screen printed electrode based non-enzymatic glucose sensor (SPE/Fe @ ZnO), *Mater. Lett.*, 2018, **212**, 231–234.

17 S. Saisa, H. Agusnar, Z. Alfian and I. Nainggolan, Polymer of chitosan with ZnO addition to optimize high responsivity and sensitivity in Sensor Film, *AIP Conf. Proc.*, 2020, **2267**, 020054, DOI: [10.1063/5.0016439](https://doi.org/10.1063/5.0016439).

18 N. Demir, K. Atacan, M. Ozmen and S. Z. Bas, Design of a new electrochemical sensing system based on MoS₂-TiO₂/reduced graphene oxide nanocomposite for the detection of paracetamol, *New J. Chem.*, 2020, **44**, 11759–11767, DOI: [10.1039/D0NJ02298E](https://doi.org/10.1039/D0NJ02298E).

19 M. A. Pellitero, Á. Colina, R. Villa and F. J. del Campo, Antimony tin oxide (ATO) screen-printed electrodes and their application to spectroelectrochemistry, *Electrochem. Commun.*, 2018, **93**, 123–127, DOI: [10.1016/j.elecom.2018.06.012](https://doi.org/10.1016/j.elecom.2018.06.012).

20 S. A. Leau, C. Lete, M. Marin, F. J. D. Campo, I. Diaconu and S. Lupu, Electrochemical sensors based on antimony tin oxide-Prussian blue screen-printed electrode and PEDOT-Prussian blue for potassium ion detection, *J. Solid State Electrochem.*, 2023, **27**, 1755–1766.

21 Z. Lu, J. Zhang, W. Dai, X. Lin, J. Ye and J. Ye, A screen-printed carbon electrode modified with a bismuth film and gold nanoparticles for simultaneous stripping voltammetric determination of Zn(II), Pb(II) and Cu(II), *Microchim. Acta*, 2017, **184**, 4731–4740.

22 H. Huang, J. Wang, Y. Zheng, W. Bai, Y. Ma and X. Zhao, A screen-printed carbon electrode modified with bismuth nanoparticles and conjugated mesoporous polymer for simultaneous determination of Pb(II) and Cd(II) in seafood samples, *J. Food Compos. Anal.*, 2024, **125**, 105837, DOI: [10.1016/j.jfca.2023.105837](https://doi.org/10.1016/j.jfca.2023.105837).

23 S. M. Mali, S. S. Narwade, Y. H. Navale, S. B. Tayade, R. V. Digraskar, V. B. Patil, A. S. Kumbhar and B. R. Stahe, Heterostructural cuo-zno nanocomposites: A highly selective chemical and electrochemical NO₂ sensor, *ACS Omega*, 2019, **4**(23), 20129–20141, DOI: [10.1021/acsomega.9b01382](https://doi.org/10.1021/acsomega.9b01382).

24 T. H. Tran and V. T. Nguyen, Copper Oxide Nanomaterials Prepared by Solution Methods, Some Properties, and Potential Applications: A Brief Review, *Int. Scholarly Res. Not.*, 2014, 1–14, DOI: [10.1155/2014/856592](https://doi.org/10.1155/2014/856592).

25 M. A. Baqya, A. Y. Nugraheni, W. Islamiyah, A. F. Kurniawan, M. M. Ramli, S. Yamaguchi, Y. Furukawa, S. Soontaranon, E. G. R. Putra, Y. Cahyono, R. Risdiana and D. Darminto, Structural study on graphene-based particles prepared from old coconut shell by acid-assisted mechanical exfoliation, *Adv. Powder Technol.*, 2020, **31**(5), 2072–2078, DOI: [10.1016/j.apt.2020.02.039](https://doi.org/10.1016/j.apt.2020.02.039).

26 P. W. Albers, V. Leich, A. J. Ramirez-Cuesta, Y. Cheng, J. Honig and S. F. Parker, The characterisation of commercial 2D carbons: graphene, graphene oxide and reduced graphene oxide, *Mater. Adv.*, 2022, **3**(6), 2810–2826, DOI: [10.1039/D1MA01023A](https://doi.org/10.1039/D1MA01023A).

27 L. Li, T. Wang, Y. Zhong, R. Li, W. Deng, X. Xiao, Y. Xu, J. Zhang, X. Hu and Y. Wang, A review of nanomaterials for biosensing applications, *J. Mater. Chem. B*, 2024, **12**(5), 1168–1193, DOI: [10.1039/D3TB02648E](https://doi.org/10.1039/D3TB02648E).

28 A. Sembiring, I. Nainggolan and A. Andriayani, Preparation and Characterization of Chitosan/Reduced Graphene Oxide Film as a Sensing Material, *J. Technomaterial Phys.*, 2023, **5**(2), 93–98, DOI: [10.32734/jotp.v5i2.13306](https://doi.org/10.32734/jotp.v5i2.13306).

29 A. Annu and A. N. Raja, Recent development in chitosan-based electrochemical sensors and its sensing application, *Int. J. Biol. Macromol.*, 2020, **164**, 4231–4244, DOI: [10.1016/j.ijbiomac.2020.09.012](https://doi.org/10.1016/j.ijbiomac.2020.09.012).

30 I. Nainggolan, S. J. Martina, S. Alva, B. Li, T. I. Nasution, A. Sembiring, A. S. Duha, S. Saisa, R. Rahman and R. Asrosa, Sensitivity of chitosan/reduced graphene oxide/manganese dioxide modified electrodes for cholesterol detection using cyclic voltammetry, *S. Afr. J. Chem. Eng.*, 2024, **48**, 329–336, DOI: [10.1016/j.sajce.2024.03.009](https://doi.org/10.1016/j.sajce.2024.03.009).

31 I. Nainggolan, S. Saisa, H. Agusnar, Z. Alfian, S. Alva, T. I. Nasution, R. Rahman and A. Sembiring, Sensitivity of chitosan film based electrode modified with reduced graphene oxide (rGO) for formaldehyde detection using cyclic voltammetry, *S. Afr. J. Chem. Eng.*, 2024, **48**, 184–193, DOI: [10.1016/j.sajce.2024.02.001](https://doi.org/10.1016/j.sajce.2024.02.001).

32 A. Aljuhani, S. M. Riyadh and K. D. Khalil, Chitosan/CuO nanocomposite films mediated regioselective synthesis of 1,3,4-trisubstituted pyrazoles under microwave irradiation, *J. Saudi Chem. Soc.*, 2021, **25**(8), 101276, DOI: [10.1016/j.jscs.2021.101276](https://doi.org/10.1016/j.jscs.2021.101276).

33 I. Nainggolan, S. Saisa, H. Agusnar, Z. Alfian, S. Alva, T. I. Nasution, R. Rahman and A. Sembiring, Sensitivity of chitosan film based electrode modified with reduced graphene oxide (rGO) for formaldehyde detection using cyclic voltammetry, *S. Afr. J. Chem. Eng.*, 2024, **48**, 184–193, DOI: [10.1016/j.sajce.2024.02.001](https://doi.org/10.1016/j.sajce.2024.02.001).

34 N. Elgrishi, K. J. Rountree, B. D. McCarthy, E. S. Rountree, T. T. Eisenhart and J. L. Dempsey, A Practical Beginner's Guide to Cyclic Voltammetry, *J. Chem. Educ.*, 2018, **95**(2), 197–206, DOI: [10.1021/acs.jchemed.7b00361](https://doi.org/10.1021/acs.jchemed.7b00361).



35 S. J. Theresa, B. Geetha, L. Deevakar and P. N. Deepa, Investigating electrochemical sensing properties of PIGE/rGO/Cu@nHAp for dynamic detection of urea, *J. Mater. Sci.: Mater. Electron.*, 2024, **35**, 1–12, DOI: [10.1007/s10854-024-12947-0](https://doi.org/10.1007/s10854-024-12947-0).

36 P. R. S. Baabu, M. B. Gumpu, N. Nesakumar, J. B. B. Rayappan and A. J. Kulandaivasamy, Electroactive Manganese Oxide–Reduced Graphene Oxide Interfaced Electrochemical Detection of Urea, *Water, Air, Soil Pollut.*, 2020, **231**(545), DOI: [10.1007/s11270-020-04899-y](https://doi.org/10.1007/s11270-020-04899-y).

37 H. S. Magar, R. Y. A. Hassan and M. N. Abbas, Non-enzymatic disposable electrochemical sensors based on CuO/Co₃O₄@MWCNTs nanocomposite modified screen-printed electrode for the direct determination of urea, *Sci. Rep.*, 2023, **13**(2034), 1–16, DOI: [10.1038/s41598-023-28930-4](https://doi.org/10.1038/s41598-023-28930-4).

38 B. J. Sanghavi, O. S. Wolfbeis, T. Hirsch and N. S. Swami, Nanomaterial-based electrochemical sensing of neurological drugs and neurotransmitters, *Microchim. Acta*, 2015, **182**(1), 1–41, DOI: [10.1007/s00604-014-1308-4](https://doi.org/10.1007/s00604-014-1308-4).

39 J. F. Patzer, S. K. Wolfson and S. J. Yao, Reactor control and reaction kinetics for electrochemical urea oxidation, *Chem. Eng. Sci.*, 1990, **45**(8), 2777–2784, DOI: [10.1016/0009-2509\(90\)80170-J](https://doi.org/10.1016/0009-2509(90)80170-J).

40 I. Naz, A. Tahira, A. A. Shah, M. A. Bhatti, I. A. Mahar, M. P. Markhand, G. M. Mastoi, A. Nafady, S. S. Medany, E. A. Dawi, L. M. Saleem, B. Vigolo and Z. H. Ibupoto, Green Synthesis of NiO Nanoflakes Using Bitter Gourd Peel, and Their Electrochemical Urea Sensing Application, *Micromachines*, 2023, **14**(3), 677, DOI: [10.3390/mi14030677](https://doi.org/10.3390/mi14030677).

41 D. Dhinasekaran, P. Soundharraj and M. Jagannathan, Hybrid ZnO nanostructures modified graphite electrode as an efficient urea sensor for environmental pollution monitoring, *Chemosphere*, 2022, **296**, 133918, DOI: [10.1016/j.chemosphere.2022.133918](https://doi.org/10.1016/j.chemosphere.2022.133918).

42 F. Zhang, M. Wang, L. Zhang and X. Su, Ratiometric fluorescence system for pH sensing and urea detection based on MoS₂ quantum dots and 2,3-diaminophenazine, *Anal. Chim. Acta*, 2019, **1077**(24), 200–207, DOI: [10.1016/j.aca.2019.06.001](https://doi.org/10.1016/j.aca.2019.06.001).

43 K. B. Babitha, P. S. Soorya, A. Peer Mohamed, R. B. Rakhi and S. Ananthakumar, Development of ZnO@rGO nanocomposites for the enzyme free electrochemical detection of urea and glucose, *Mater. Adv.*, 2020, **1**(6), 1939–1951, DOI: [10.1039/DOMA00445F](https://doi.org/10.1039/DOMA00445F).

44 A. Bard and L. Faulkner, *Electrochemical Methods : Fundamentals and Application*, John Wiley & Sons Inc, United States, 2001.

45 R. Ahmad, N. Tripathy and Y. B. Hahn, Highly stable urea sensor based on ZnO nanorods directly grown on Ag/glass electrodes, *Sens. Actuators, B*, 2014, **194**, 290–295, DOI: [10.1016/j.snb.2013.12.098](https://doi.org/10.1016/j.snb.2013.12.098).

46 M. Rafiq, A. Siddique, M. F. Rabbee, S. M. S. Jillani, J. Y. G. Al-Humaidi, A. Dildar, M. T. Qamar, S. K. Haider, M. D. Akhtar, M. A. Fazal, M. A. Khan, M. M. R. Khan, T. A. Sheikh and M. M. Rahman, Sensitive detection of urea based on Dy₂O₃–Co₃O₄@ZrO₂ nanocomposite by electrochemical approach for environmental assessment, *Microchem. J.*, 2024, **207**, 111915, DOI: [10.1016/j.microc.2024.111915](https://doi.org/10.1016/j.microc.2024.111915).

